Kapal: Jurnal Ilmu Pengetahuan dan Teknologi Kelautan
(Kapal: Journal of Marine Science and Technology)
journal homepage : http://ejournal.undip.ac.id/index.php/kapal
2301-9069 (e)
1829-8370 (p)

Hydrodynamic Forces on Submerged Floating Tube: The Effect of Curvature Radius and Depth Level

Jamiatul Akmal[1)*], Asnawi Lubis[1)], Ahmad Su'udi[1)], Novri Tanti[1)], Nurcahya Nugraha[1)]
Zaky Abyan Fahrain[1)], Panji Firmanul Hakim[1)]

[1)] Department of Mechanical Engineering, Universitas Lampung, Lampung, Indonesia
[*)] Corresponding Author: jamiatul.akmal@eng.unila.ac.id

Article Info

Keywords:
SFTB; wave; curvature radius; depth level; hydrodynamic forces

Article history:
Received: 09/01/2022
Last revised: 10/02/2022
Accepted: 14/02/2022
Available online: 14/02/2022
Published: 28/02/2022

DOI:
https://doi.org/10.14710/kapal.v19i3.44019

Abstract

The discussion of hydrodynamic forces becomes an important issue in determining the dynamic behavior of the Submerged Floating Tunnel Bridge (SFTB) structure. As stated in the Morison Equation, the hydrodynamic forces are affected by the kinematics of water particles, but up to this date, there are only a few discussions for curved tube applications. This paper discusses the effect of curvature radius and depth level on hydrodynamic forces to get the correction factor for a straight tube. Tubes with variations in radius curvature (R/L) and diameter (D) were installed in a wave pool with a depth level (z/d). The hydrodynamic forces were detected by a load cell sensor placed on a pedestal at the end of the specimen. The data from the load cell was processed by the data acquisition system and displayed on the monitor screen, showing that the z/d ratio and the R/L ratio both affect the hydrodynamic forces. A larger z/d ratio (deeper) results in smaller hydrodynamic forces, while a smaller R/L ratio (more curved) results in smaller hydrodynamic forces. A correction factor (C) has been determined to calculate the hydrodynamic force on a curved tube based on the Morison equation.

1. Introduction

Tubular structures are commonly used in maritime structures, such as; structural support poles [1], submarine cable lines [2], oil and gas pipelines [3, 4], mooring cables for Tension Leg Platform/TLP [5], and so on. Today, the use of this structure has developed into various fields and requires increasingly complex studies. For example, the use of this structure is being studied for application as a submerged floating tunnel bridge/SFTB [6, 7]. One important issue that needs to be discussed is the hydrodynamic force. This force occurs due to the interaction between the fluid and the tubular structure through the waves. The analysis is developed based on theoretical approaches to defining the various type of waves, including small-amplitude wave theory and finite wave theory [8, 9].

The hydrodynamic forces are affected by the KC number and the drag coefficient, C_D [10]. The KC number is the ratio of the wave motion to the cylinder diameter, while the C_D value depends on the geometry and Reynolds number. This theory has been proved analytically and numerically [11, 12]. One example of the application of the KC number is to calculate the hydrodynamic force on a pipeline on the seabed using the Wake II Model, which was adopted for the analysis of lift force, drag force, inertia force and the total hydrodynamic force. This equation can predict the hydrodynamic force accurately [13].

The hydrodynamic forces consist of two components; the drag and the inertial force, each affected by the velocity and acceleration of the water particles, as proposed by Morison, well known as Morison Equation [14, 15]. Morison Equation is effectively used to predict the hydrodynamic forces on a vertically or horizontally installed tube [16]. The numerical study of the hydrodynamic forces on a floating tube subjected to internal solitary waves also proves the accuracy of this equation [17, 18].

In certain constructions, a curved tubular structure is required for several technical reasons, such as the Submerged Floating Tunnel Bridge/SFTB [19]. One of the reasons for using a curved tubular structure is to gain flexibility during operation, especially anticipating changes in length caused by temperature differences [20]. Flexibility is needed to reduce cyclic loads that can cause fatigue failure in structures [21, 22]. The curved cylindrical construction also improves stability by increasing stiffness to reduce lateral movement. However, there is not much research on hydrodynamic forces on the curved tubular structure yet. For this reason, this article discusses the effect of the degree of curvature on the hydrodynamic forces that occur. The study was conducted to obtain a correction factor C to calculate the hydrodynamic force on a curved tube based on the Morison equation.

2. Methods

The research was conducted on an experimental pool, which is a modified model from our previous research [23], as shown in Fig. 1. Specimens are made of tubes with varying degrees of curvature, being assembled on a holder frame. At both ends of the specimen, the supports are equipped with load cells to measure the force received by the waves. The signal from the loadcell is read by a set of data acquisition system tools. Fig. 2 shows the design of the specimens with variations in the degree of curvature (*R/L*) and their sizes are shown in Table 1. The specimens are placed with varying degrees of depth (*z/d*).

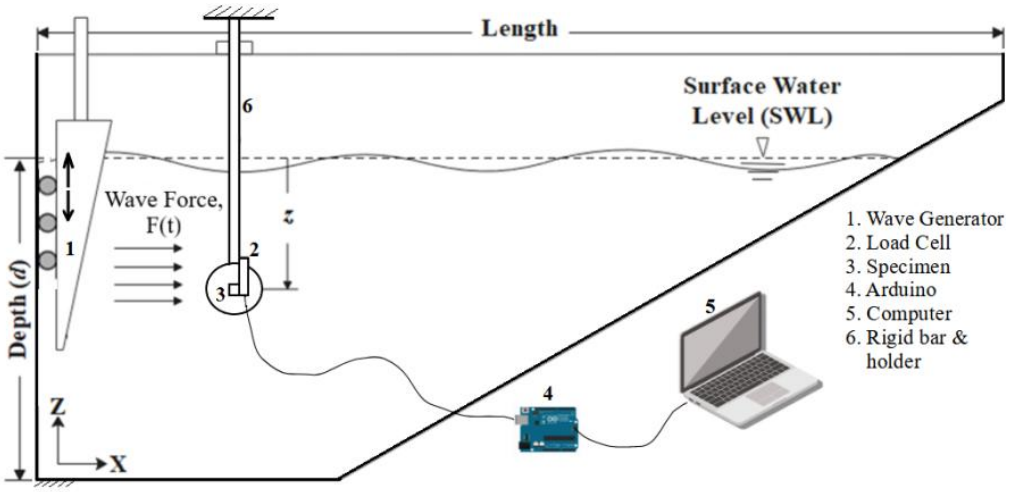

Figure 1. Experimental pool set-up [23]

Tabel 1. Specimen specifications

Radius curvature, *R* mm	Tube length, *L* mm	Ratio, *R/L*	Tube Diameter, *D* inch (mm)	Total depth (mm)	Depth level, *z/d*
∞ (straight)	500	-	1 (25.4)	600	1/6
400		0.8	1,5 (38.1)		2/6
600		1.2	2 (50.8)		3/6
800		1.6	2,5 (63.5)		
1000		2	3 (76.2)		
1200		2.4			

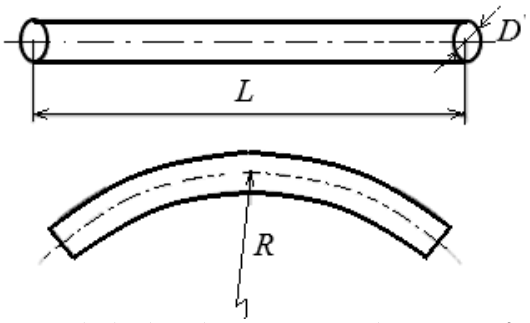

Figure 2. Specimens (tubes) with variations in the degree of curvature (*R/L*)

2.1. Kinematics of Water Particles and Hydrodynamic Forces

In this research, wave characteristics were developed based on Airy's theory. This theory is considered the most relevant because the waves that occur are relatively small and conform to Eq. (1), where η_0 is the wave amplitude and H is the total wave height, as shown in Fig. 3. The motion of water particles can be determined from the potential velocity using the Laplace equation, as shown in Eq. (2) [24]. Here, the *x*-axis represents a horizontal direction, while the *z*-axis represents a vertical direction.

$$\frac{\eta_0}{H} \langle 0.5 \tag{1}$$

$$\frac{\partial^2 \phi}{\partial x^2} + \frac{\partial^2 \phi}{\partial z^2} = 0 \tag{2}$$

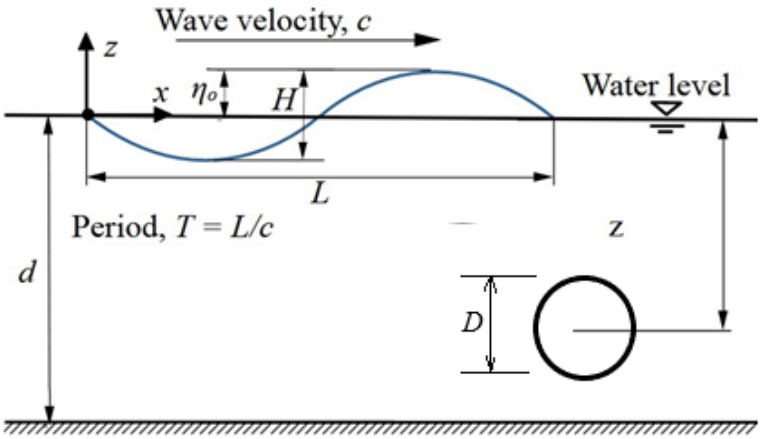

Figure 3. Wave and Specimen Specifications

Setting the boundary conditions on the seabed (at z/d=1), $\partial\phi/\partial z$=0, the solution for potential velocity can be solved by the variable separation method, as shown in Eq. (3). Here, k is the wavenumber, as shown in Eq. (4).

$$\phi = \frac{\pi H}{kT}\frac{\cosh\left[k\left(z+d\right)\right]}{\sinh\left(kd\right)}\sin\left(kx-\omega t\right) \tag{3}$$

$$k = \frac{2\pi}{L} \tag{4}$$

The velocity and acceleration of water particles for various depth levels based on Airy's theory can be seen in Eq. (5) and Eq. (6), respectively [25].

$$u = \frac{\pi H}{T}\frac{\cosh\left[k\left(z+d\right)\right]}{\sinh\left(kd\right)}\sin\theta \tag{5}$$

$$\dot{u} = \frac{-2\pi H}{T^2}\frac{\cosh\left[k\left(z+d\right)\right]}{\sinh\left(kd\right)}\cos\theta \tag{6}$$

The hydrodynamic force is obtained from the Morison Equation, as shown in Eq. (7), where C_D is the coefficient of drag, Cm is the coefficient of inertia, ρ is water density, D is tube diameter, u and $\dot{u}$ is velocity and acceleration, respectively, as shown in Eq. (5) and Eq. (6).

$$f\left(t\right) = \frac{1}{2}C_D\rho u|u| + C_m\frac{\rho\pi D^2}{4}\dot{u} \tag{7}$$

2.2. Numerical Analysis

The parameters used in the numerical analysis are the same as the specifications on the experimental equipment. The analysis stages consist of preprocessing, solution, and postprocessing. In the preprocessing stage, geometry and meshing are made. In the solution stage, boundary conditions and mechanical properties of the material are defined. The results of the analysis are presented in the Postprocessing stage.

The numerical analysis is modeled as Volume of Fluid (VoF)-Open Channel Wave BC. The meshing element size is 30 mm with a Quadrilateral/Hexahedron shape. There are four boundary conditions; Cylinder Wall (Wall), Channel Wall (Wall), Inlet (Velocity Inlet), and Outlet (Pressure Outlet), as shown in Fig. 4.

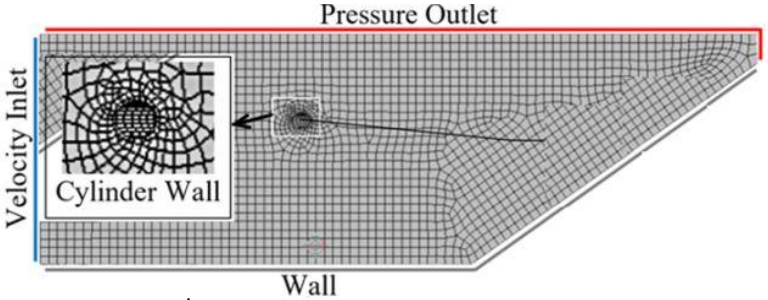

Figure 4. Meshing element and boundary conditions

2.3. Experimental set up

The experiment was carried out in an experimental pool equipped with a set of wave generators, as shown in Fig. 5. The dimensions of the pool and the characteristics of the waves are shown in Table 2.

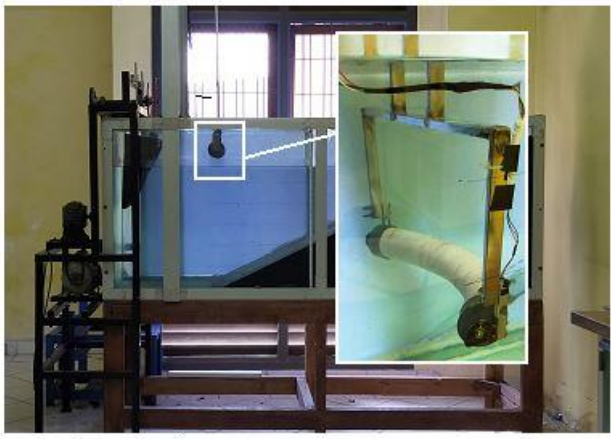

Figure 5. Test equipment settings

Tabel 2. The dimensions of the pool and the characteristics of the waves

Description	Symbol	unit	Value
Length		mm	2000
Wide		mm	600
Depth	d	mm	600
Wave direction	$F(t)$		x-direction
Excitation frequency	ω	Hz (rad/s)	1,55 (9,77)
Wave Height	H	mm	23
Wavelength	L	mm	558

3. Results And Discussion

In this section, research results will be presented and discussed, including; velocity and acceleration of water particles and their effect on hydrodynamic forces. Then discussed the effect of curvature, the effect of depth level and the effect of tube diameter on the hydrodynamic force.

3.1. Profile graph of velocity and acceleration of water particles

At the surface of the water, the velocity and acceleration of the water particles are relatively larger than those in deeper positions. These profiles are obtained from solving Equations (2) and (3), respectively. Based on this graph, at depths z=-0.2 to z=-0.6 (z/d=1/3 to z/d=1), the rate of reduction of the hydrodynamic force does not change significantly. Thus, it can be recommended that the optimum placement for SFTB is at the level of z/d=1/3, as shown in Fig. 6 (a) and (b).

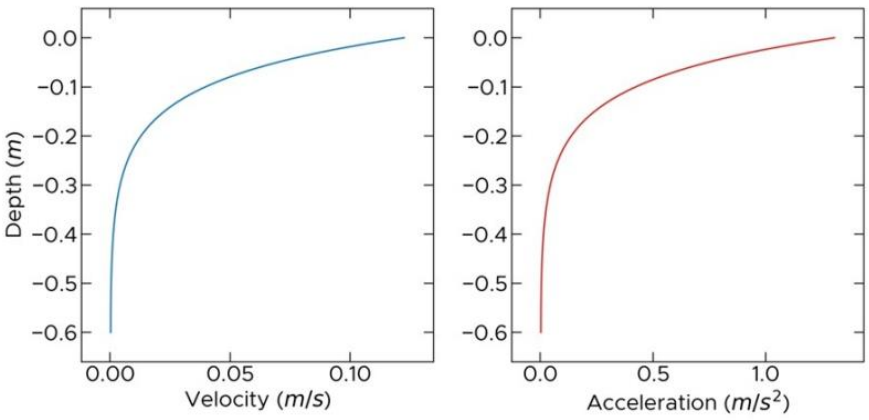

(a) (b)

Figure 6. Fluid particle kinematics (a) Velocity and (b) Acceleration

3.2. Verification of hydrodynamic force on straight tube

Fig. 7 shows the hydrodynamic force on a straight tube obtained experimentally and numerically. The analytical solution of the Morison Equation is also shown for comparison. Visually, all the graphs tend to have the same trend, although there are slight inaccuracies. The numerical graph is relatively more precise than the experimental one, compared to Morison's graph. The experimental graph is relatively higher than Morison's graph near the water surface (z/d=1/6). Otherwise, it is

lower at the deeper position (z/d=3/6). It is due to the wave generator's closer placement to the surface and causes it unable to reach the pool's bottom. In future research, the difference of the domain between experimental and numerical can be solved by improving the design of the wave generator to get more accurate results.

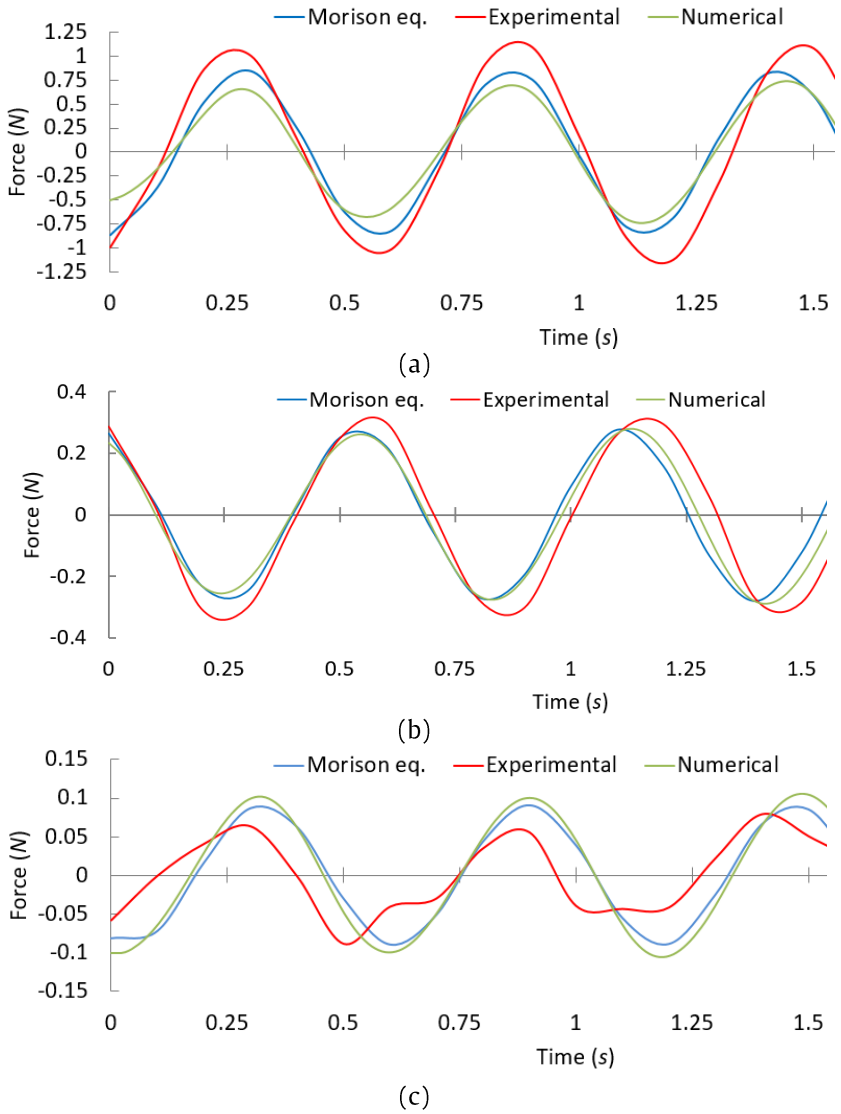

Figure 7. Hydrodynamic forces: (a) depth level z/d=1/6, (b) depth level z/d=2/6, and (c) depth level z/d=3/6

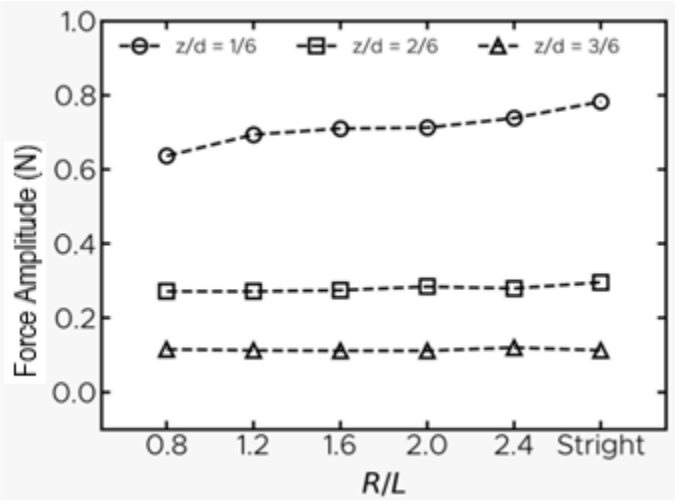

Figure 8. Effect of curvature radius on hydrodynamic force

3.3. Effect of Curvature radius on Hydrodynamic Force

The hydrodynamic forces on the specimen are corrected by the curvature radius R/L, where the smaller R/L ratio given will results in the smaller amount of forces received, as shown in Fig. 8. If the Morison Equation applied to a straight tube is considered a reference, multiplying it by the correction factor (C) will make it applicable for a curved tube. The correction

factor (C) in each variation of curvature radius for the most recommended depth level (z/d=1/3) based on Fig. 6 is served in Table 3. This correction factor is calculated numerically, which is considered relatively more accurate. The value of C is calculated based on the ratio of the hydrodynamic force on the curved tube to the hydrodynamic force of the straight tube. Thus, Equation (7) can be modified to calculate the Morison force on a curved tube, as shown in Eq. (8).

$$f\left(\frac{R}{L}\right) = C\left(\frac{1}{2}C_D\rho u|u| + C_m\frac{\rho\pi D^2}{4}\dot{u}\right) \quad (8)$$

Tabel 3. The correction factor for variations in the curvature radius at optimal placement (z/d = 1/3)

R/L	Hydrodynamic Force (N)	Correction Factor, *C*
∞(Straight)	0.296	1
0.8	0.284	0.96
1.2	0.279	0.94
1.6	0.275	0.92
2	0.272	0.91
2.4	0.272	0.91

3.4. Effect of depth level on hydrodynamic forces

Fig. 9 shows the depth level' s effect on the hydrodynamic force amplitude, both experimentally and numerically. Placing the specimen at a high depth level further reduces the amplitude of the hydrodynamic force. This result is in good agreement with the Morison force equation (Equation 4), where the hydrodynamic forces are directly proportional to the velocity and acceleration of the water particles. In the kinematics equation of water particles as stated in Equation (2) and Equation (3), it can be seen that at deeper positions, the velocity and acceleration of water particles become smaller. The ratio of curvature (R/L) affects the drag coefficient (C_D) in the Morison Equation. Smaller R/L value will produce smaller C_D coefficient, thus reducing the hydrodynamic force.

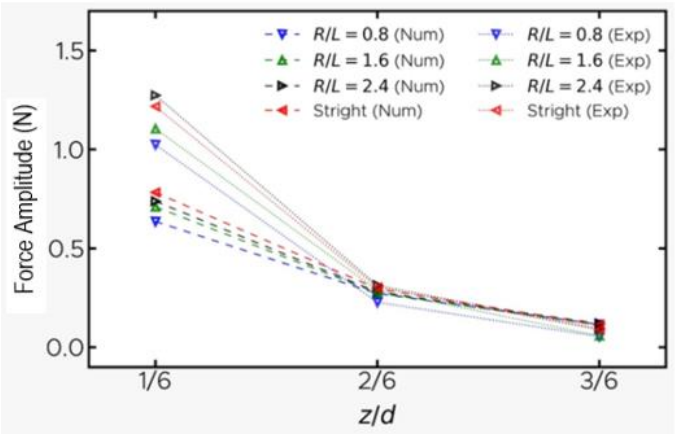

Figure 9. Effect of depth level on hydrodynamic forces

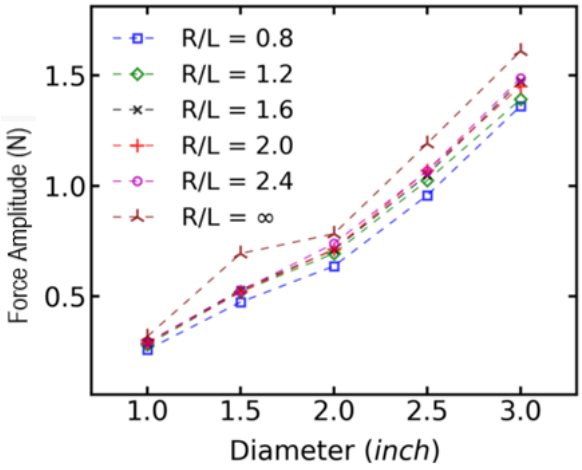

Figure 10. Effect of tube diameter on hydrodynamic forces

3.5. Effect of tube diameter on hydrodynamic forces

Fig. 10 shows the tube diameter's effect on the hydrodynamic forces' amplitude, numerically. The diameter of the tube is directly proportional to the hydrodynamic forces it receives. This corresponds with the Morison Force Equation (Equation 7): the larger the diameter, the greater the drag and inertia forces received. In addition, the curvature ratio (R/L) affects the hydrodynamic forces, in agreement with those discussed in section 3.4.

4. Conclusion

The hydrodynamic forces are influenced by depth level, curvature radius, and tube diameter. The hydrodynamic forces are the greatest near the water surface (z/d=0) and will gradually decrease at a deeper position until the bottom of the pool (z/d=1). The rate of reduction of the hydrodynamic forces is not linear but satisfies a hyperbolic function. At the depth level z/d≈1/3 to z/d=1, the hydrodynamic forces are not significantly reduced. Thus, we recommend z/d≈1/3 is optimal for SFTB placement. In addition, the smaller the curvature radius (R/L), the smaller the hydrodynamic force. A correction factor, C, has been determined to calculate the hydrodynamic force on a curved tube based on the Morison equation which applies to a straight tube.

Acknowledgment

The authors would like to acknowledge Universitas Lampung, for founding this research under the scheme of Hibah Pascasarjana, SPK: 1543/UN26.21/PN/2021, Date 21 April 2021.

References

[1] A. Malekjafarian, S. Jalilvand, P. Doherty, and D. Igoe, "Foundation Damping for Monopile Supported Offshore Wind Turbines: A Review," *Marine Structure*, vol. 77, p. 102937, 2021. doi: 10.1016/j.marstruc.2021.102937

[2] F. Dinmohammadi *et al.*, "Predicting Damage and Life Expectancy of Subsea Power Cables in Offshore Renewable Energy Applications," *IEEE Access*, vol. 7, pp. 54658–54669, 2019. doi: 10.1109/ACCESS.2019.2911260.

[3] X. Cheng, Y. Wang, and G. Wang, "Hydrodynamic Forces on a Large Pipeline and a Small Pipeline in Piggyback Configuration under Wave Action," *Journal Waterway Port Coastal Ocean Engineering*, vol. 138, no. 5, pp. 394–405, 2012. doi: 10.1061/(ASCE)WW.1943-5460.0000144

[4] N. J. Shankar, H.-F. Cheong, and K. Subbiah, "Wave Force Coefficients for Submarine Pipelines," *Journal Waterway Port Coastal Ocean Engineering*, vol. 114, no. 4, pp. 472–486, 1988. doi: 10.1061/(ASCE)0733-950X(1988)114:4(472)

[5] J. Yu, S. Hao, Y. Yu, B. Chen, S. Cheng, and J. Wu, "Mooring Analysis for a Whole TLP with TTRs under Tendon One-Time Failure and Progressive Failure," *Ocean Engineering*, vol. 182, pp. 360–385, 2019.doi: 10.1016/j.oceaneng.2019.04.049

[6] S. Seo, H. Mun, J. Lee, and J. Kim, "Simplified Analysis for Estimation of the Behavior of a Submerged Floating Tunnel in Waves and Experimental Verification," *Marine Structure*, vol. 44, pp. 142–158, 2015. doi: 10.1016/j.marstruc.2015.09.002

[7] M. Sharma, R. B. Kaligatla, and T. Sahoo, "Wave Interaction with a Submerged Floating Tunnel in the Presence of a Bottom Mounted Submerged Porous Breakwater," *Applied Ocean Research*, vol. 96, p. 102069, 2020. doi: 10.1016/j.apor.2020.102069

[8] R. G. Dean and R. A. Dalrymple, *Water Wave Mechanics for Engineers and Scientists*, vol. 2. World Scientific Publishing Company, 1991.

[9] R. M. Sorensen, *Basic Coastal Engineering*, vol. 10. Springer Science & Business Media, 2005.

[10] T. Sarpkaya, "Force on a Circular Cylinder in Viscous Oscillatory Flow at Low Keulegan–Carpenter Numbers," *Journal of Fluid Mechanics*, vol. 165, pp. 61–71, 1986. doi: 10.1017/S0022112086002999

[11] Y. Li and M. Lin, "Hydrodynamic Coefficients Induced by Waves and Currents for Submerged Circular Cylinder," *Procedia Engineering*, vol. 4, pp. 253–261, 2010. doi: 10.1016/j.proeng.2010.08.029

[12] V. Venugopal, K. S. Varyani, and P. C. Westlake, "Drag and Inertia Coefficients for Horizontally Submerged Rectangular Cylinders in Waves and Currents," *Proceedings of the Institution of Mechanical Engineers. Part M J. Eng. Marit. Environ.*, vol. 223, no. 1, pp. 121–136, 2009.

[13] I. Iyalla, M. Hossain, and J. Andrawus, "Calculating Hydrodynamic Loads on Pipelines and Risers: Practical Alternative to Morison′ s Equation," in *Advanced Materials Research*, 2012, vol. 367, pp. 431–438. doi: 10.4028/www.scientific.net/AMR.367.431

[14] H. Kunisu, "Evaluation of Wave Force Acting on Submerged Floating Tunnels," *Procedia Engineering*, vol. 4, pp. 99–105, 2010. doi: 10.1016/j.proeng.2010.08.012

[15] J. R. Morison, J. W. Johnson, and S. A. Schaaf, "The Force Exerted by Surface Waves on Piles," *Journal of Petrolium Technology*, vol. 2, no. 05, pp. 149–154, 1950. doi: 10.2118/950149-G

[16] P. Boccotti, F. Arena, V. Fiamma, and A. Romolo, "Two Small-Scale Field Experiments on the Effectiveness of Morison′ s Equation," *Ocean Engineering*, vol. 57, pp. 141–149, 2013. doi: 10.1016/j.oceaneng.2012.08.011

[17] X. Zan and Z. Lin, "On the Applicability of Morison Equation to Force Estimation Induced by Internal Solitary Wave on Circular Cylinder," *Ocean Engineering*, vol. 198, p. 106966, 2020. doi: 10.1016/j.oceaneng.2020.106966

[18] S. Zhang, C. Chen, Q. Zhang, D. Zhang, and F. Zhang, "Wave Loads Computation for Offshore Floating Hose Based on Partially Immersed Cylinder Model of Improved Morison Formula," The *Open Petroleum Engineering Journal*, vol. 8, no. 1, 2015. doi: 10.2174/1874834101508010130

[19] B. Jakobsen, "Design of the Submerged Floating Tunnel Operating under Various Conditions," *Procedia Engineering*, vol. 4, pp. 71–79, 2010. doi: 10.1016/j.proeng.2010.08.009

[20] E. M. M. Fonseca, F. De Melo, and C. A. M. Oliveira, "The Thermal and Mechanical Behaviour of Structural Steel Piping Systems," *International Journal of Pressure Vessels and Piping*, vol. 82, no. 2, pp. 145–153, 2005. doi: 10.1016/j.ijpvp.2004.06.012

[21] M. Ali Ghaffari and H. Hosseini-Toudeshky, "Fatigue Crack Propagation Analysis of Repaired Pipes with Composite Patch under Cyclic Pressure," *Journal of Pressure Vessel Technology*, vol. 135, no. 3, p. 031402, 2013. doi: 10.1115/1.4023568

[22] A. Samanci, A. Avci, N. Tarakcioglu, and Ö. S. Şahin, "Fatigue Crack Growth of Filament Wound GRP Pipes with a Surface Crack under Cyclic Internal Pressure," *Journal of Material Science*, vol. 43, no. 16, pp. 5569–5573, 2008. doi: 10.1007/s10853-008-2820-x
[23] J. Akmal, A. Lubis, N. Tanti, N. Nuryanto, and A. W. Murti, "The TLP 2-DOF as an Alternative Model for Extreme Wave Application," *Kapal: Jurnal Ilmu Pengetahuan dan Teknologi Kelautan*, vol. 18, no. 2, pp. 80–87, 2021. doi: 10.14710/kapal.v18i2.37187
[24] T. Sarpkaya, *Wave Forces on Offshore Structures*. Cambridge university press, 2010.
[25] V. Sundar, *Ocean Wave Mechanics: Applications in Marine Structures*. John Wiley & Sons, 2017.